

## EXPERIMENTAL AND SIMULATION STUDY OF HYBRID GROUND-SOURCE HEAT PUMP SYSTEMS WITH UNGLAZED SOLAR COLLECTORS FOR FRENCH OFFICE BUILDINGS

Vincent Helpin<sup>1</sup>, Michaël Kummert<sup>1</sup>, and Odile Cauret<sup>2</sup>

<sup>1</sup>Department of Mechanical Engineering, École Polytechnique de Montréal, QC, Canada

<sup>2</sup>Department "Energy in buildings and territories", EDF R&D, France

### ABSTRACT

This paper discusses the potential of a Solar Assisted Ground-Source Heat Pump (SAGSHP) system configuration with unglazed solar collectors to supply space heating in French office buildings, with reduced capital cost.

Experimental results are used to develop validated TRNSYS component models for the unglazed solar collectors and the heat pump. A complete TRNSYS model (system and building) is then developed to assess the potential of this SAGSHP configuration in a typical office building in France.

Results show that coupling unglazed solar collectors with ground heat exchangers is potentially interesting in terms of capital costs as well as in improvement of performance.

### INTRODUCTION

Ground Source Heat Pumps (GSHP) are widely in use throughout the world to provide heating and cooling, and they have demonstrated interesting energy savings compared to more common systems like gas boilers. However, their market share is still limited by high capital costs compared to many competing technologies. The cost for the ground heat exchanger (GHX), i.e. drilling (or trenching), piping and backfilling, is often the most significant contributor to capital costs. In France, like in Germany (Blum et al. 2011), the average contribution of borehole costs is about 50% of the total, with an average cost of 100 €/m (including connection to the heat pump).

In heating-only or heating-dominated applications, the yearly load imbalance leads to ground cooling over the years. The borehole length must be increased to cope with that fact, especially in larger systems with multiple boreholes that thermally interact with each other. Supplemental heat sources such as solar collectors have the potential to reduce the required length of ground heat exchanger, hence the capital cost.

Although hybrid ground-source heat pump systems (HyGSHP) have been mostly studied in cooling-dominated cases (where a supplemental heat rejector such as a cooling tower is added to the GHX loop),

heating-dominated systems have received some attention in the literature in the past few years.

Chiasson and Yavuzturk (2003) performed a simulation study to assess the viability of using solar thermal collectors to balance annual ground loads and reduce capital costs. They modelled a school building with typical meteorological year weather data for six US cities and sized the system to maintain the heat pump entering water temperature (i.e. the ground return temperature) above 0 °C after 20 years of operation. Their study concludes that hybrid SAGSHP systems can reduce the system life cycle costs for locations that have high borehole heat exchanger costs.

Other studies (e.g. Rad et al., 2009) conclude that, with glazed solar collectors, the capital cost reduction is very limited. Some experimental studies were found in the literature (Ozgener and Hepbasli, 2005; Bakiri et al., 2011) but the capital cost reduction is not considered.

In order to study the potential of SAGSHP systems with unglazed collectors to reduce capital costs, a full-scale SAGSHP system was designed, implemented and investigated on a test platform at EDF R&D (Cauret and Teuillières, 2010). The study presented in this paper is based on these experimental results.

### OBJECTIVE

This study aims at assessing the potential of unglazed solar collectors to reduce the capital cost of GSHP systems in commercial buildings in France. Experimental results obtained on EDF R&D field test platform will permit to obtain validated component models for unglazed solar collectors and the heat pump. A complete TRNSYS model of a typical French office building equipped with this SAGSHP system will then be developed and used to assess the potential cost benefit of this system.

### THE TESTING FACILITY

#### **Description**

An SAGHP system was installed at EDF R&D center and connected to an existing natural climate platform. The platform is designed to test GSHP in a natural climate over one or more years. It consists of a 3000 m<sup>2</sup> area dedicated to the installation of ground

collectors and a control room equipped with heat pumps. The set-up used in the present study is shown in Figure 1. It consists of a 9 kW water-to-water heat pump connected to a ground collector field and optionally in series with a 20 m<sup>2</sup> area of unglazed solar collectors. The operation of the heat pump is driven by a control loop which mimics the operation of a real house according to real-time weather. Thus, whenever house heating is required the heat pump is activated to heat a 500 liter tank which acts as a house. The house load is rejected outside using an air cooler loop.

The ground heat exchangers are compact collectors provided by IVT Industrier AB, and previously evaluated (Cauret et al, 2009). There are 4 parallel strings of 8 compact modules, for a total pipe length of approximately 1300 m. The unglazed collectors are manufactured by the French company Heliopac (CSTB, 2008).

A total of 38 sensors have continuously recorded various experimental data during more than eleven months (November 2007 to October 2008) with a time step of one minute. Among others, the following parameters are monitored:

- Ambient air temperature ( $T_{amb}$ )
- Global Solar radiation on the horizontal ( $G_{sun}$ )
- Fluid Flow rates (source side and load side).
- The solar collector inlet and outlet temperatures
- Heat Pump leaving and entering temperatures.
- Temperatures in the ground heat exchanger loop.

The solar collectors are connected to the GHX through a motorized three-way valve. The valve directs the flow towards the solar collectors if the temperature difference between the collector outlet and the GHX outlet is higher than 0.5 °C. This limit has been determined during the first month of operation as a good value to avoid controller instability issues while considering possible effects of stagnation inside the solar collectors. When the

heat pump is off (no load) and the valve opened, a secondary pump circulates the fluid so that the ground can be recharged.

### Main Results

Preliminary tests were taking place in November so that data has been discarded. From December to the last day of heating (16<sup>th</sup> of May), the unglazed collectors have been active for 2200 hours providing 1700 kWh directly to the heat pump (the GHX provided another 8500 kWh). The solar collectors also provided 5400 kWh to the ground during periods without load.

An interesting fact is that the average solar efficiency, defined as the total energy gain divided by the total incident irradiation, would give a value higher than 1 in this case. Even during winter nights the ambient air temperature is often higher than the GHX outlet temperature as shown in Figure 2, next page. The winter irradiance is often low so the collector outlet temperature is lower than the ambient temperature and a significant part of the useful energy is gained through heat exchange with the ambient air (cf. Figure 3, next page).

The heat pump has been operating during around 2040 hours for 168 heating days. Its average Coefficient Of Performance (COP) for this period is 3.73. Ground temperatures are not discussed here since special compact ground exchangers have been tested and more usual vertical boreholes are used in the simulation study. Because some parameters such as wind speed or the dew point temperatures are not measured on the experimental facility, additional weather data was obtained from the real-time hourly weather data service provided by the US DOE (EERE, 2011). Figure 4, next page, compares the ambient temperature measurements taken on the experimental site with values at the weather station of Melun, which is located 30 km away from the EDF R&D center. The comparison shows that the weather station can provide a reasonable proxy for missing parameters.

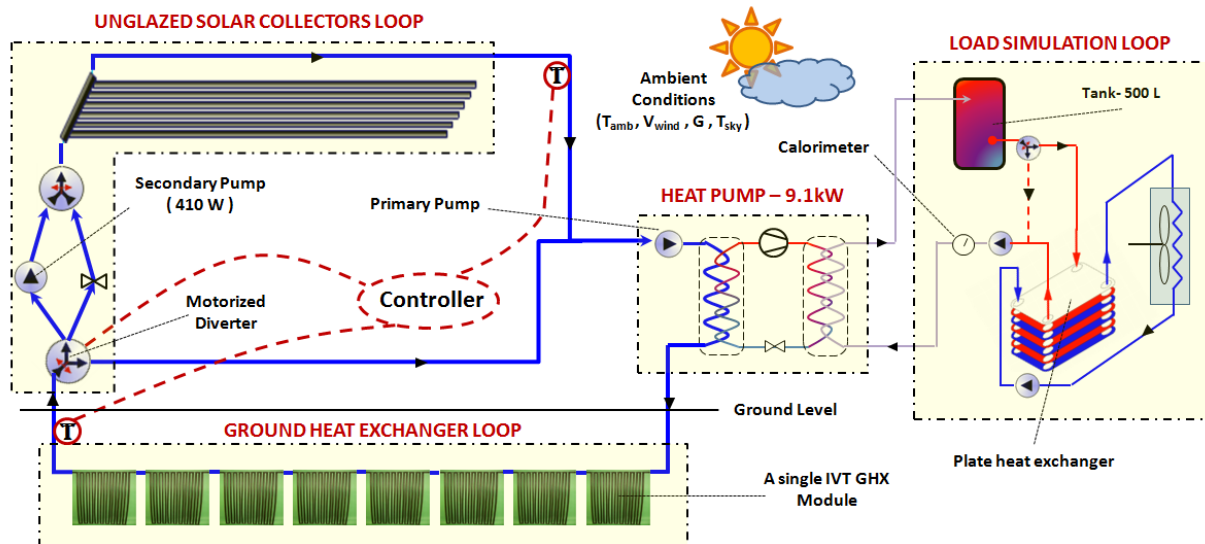


Figure 1: Schematic view of the test facility at EDF R&D Center.

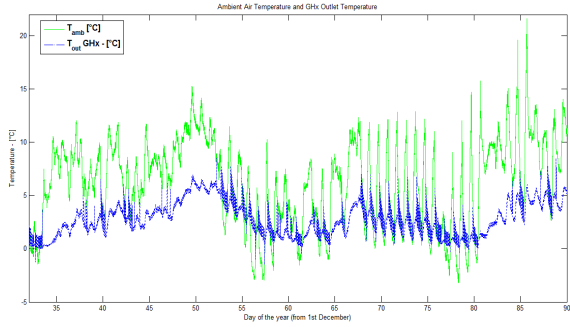


Figure 2: GHX outlet temperature ( $T_{out\_GHX}$ ) and  $T_{amb}$  during January and February 2008.

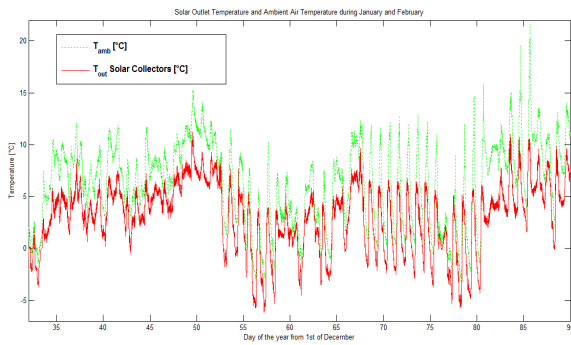


Figure 3: Collector outlet temperature and  $T_{amb}$  for January and February 2008.

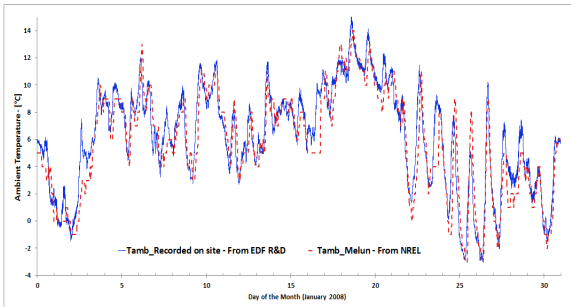


Figure 4: Ambient temperature recorded at the EDF facility and at the Melun weather station for January

## UNGLAZED SOLAR COLLECTORS MODEL VALIDATION

### Collectors Description



Figure 5: Unglazed collector mounted on the roof.

As shown in Figure 5, the solar collectors are mounted flat on a horizontal roof. Three series of 28 tubes are connected in parallel through white intake

manifolds. The black coated pipe network is made of EPDM material and has a fluid capacity of 6.6 L/m<sup>2</sup>.

### Simulation Parameters

As recalled by Burch et al (2005), the conversion efficiency equation for unglazed collectors differs from the general Hottel-Whillier form due to additional dependencies on wind speed and sky infrared radiation. The unglazed collector efficiency can be approximated by the following equations:

$$\eta = F_r(\tau\alpha)_n * K - F_r U_l * \frac{T_{in} - T_{amb}}{G_{net}} \quad (1)$$

$$F_r(\tau\alpha)_n = a_0 - a_1 * v_{wind} \quad (2)$$

$$F_r U_l = b_0 + b_1 * v_{wind} \quad (3)$$

$$G_{net} = G_{sun} + \frac{\epsilon}{\alpha} * G_L \quad (4)$$

$v_{wind}$  in Equations 2 and 3 is the local wind speed, which is different from the wind speed typically found in weather data files (measured at an airport at a height of 10 m). Although the local speed is sometimes estimated as a function of wind direction, this paper uses the same approximation as Burch et al. (2005), where the local speed is a constant fraction of the speed measured at the weather station.  $G_{sun}$  is the solar short-wave solar radiation and  $G_L$  represents the relative long wave radiation exchange between the sky and a black body at ambient temperature:

$$G_L = \sigma (T_{sky}^4 - T_{amb}^4) \quad (5)$$

The effective sky temperature can be determined from the sky emissivity in presence of clouds,  $E_{sky}$ , which is estimated from the clear sky emissivity,  $E_{o,sky}$ , and the fraction of sky covered by opaque clouds  $f_{cloud}$ . In the model,  $\epsilon_{cloud}$  is fixed to 0.45.

$$T_{sky} = E_{sky}^{\frac{1}{4}} * (T_{amb} + 273.13) - 273.13 \quad (6)$$

$$E_{sky} = E_{o,sky} + (1 - E_{o,sky}) * f_{cloud} * \epsilon_{cloud} \quad (7)$$

Berdahl and Martin (1984) provide an estimation of the clear sky emissivity based on the dew point temperature  $T_{dp}$ , the dry bulb temperature  $T_{amb}$  and the hour of the day from midnight  $t$ , with the following relation:

$$E_{o,sky} = 0.711 + 0.56 \frac{T_{dp}}{100} + 0.73 \left( \frac{T_{dp}}{100} \right)^2 + 0.013 \cos(15t) \quad (8)$$

Since there is no glazing, the incidence angle modifier  $K(\theta)$  is calculated from the ratio of solar absorptance and solar absorptance at normal incidence from Duffie and Beckman (2006):

$$\frac{\alpha}{\alpha_n} = 1 - 11.588 \cdot 10^{-3} \theta + 2.731 \cdot 10^{-4} \theta^2 - 2.302 \cdot 10^{-5} \theta^3 + 9.0244 \cdot 10^{-7} \theta^4 - 1.80 \cdot 10^{-8} \theta^5 + 1.7734 \cdot 10^{-10} \theta^6 - 6.9937 \cdot 10^{-13} \theta^7 \quad (9)$$

Table 1 shows the efficiency parameters provided in the collector test report (CSTB, 2008). Efficiency is expressed based on the gross area. The ratio between aperture area (CEN, 2005) and gross area has been estimated at 0.8 considering a space of 7.7 mm between the tubes (see Figure 6) and adding the estimated impact of inlet and outlet manifolds.

Table 1 - Collector test report efficiency parameters

Parameter	Value	Unit
$a_0$	0.608	-
$a_1$	0.0	s/m
$b_0$	16	$W/m^2 \cdot ^\circ C$
$b_1$	3.2	$J/m^3 \cdot ^\circ C$
$\epsilon$	0.9	-
$\alpha$	0.9	-

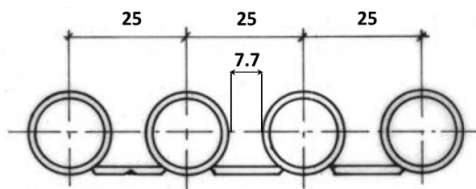


Figure 6: Sectional view of 4 collector pipes with spacers (CSTB, 2008).

Only the fluid thermal mass is taken into account (550 kJ/K for 20 m<sup>2</sup>). The nominal fluid flow rate is equal to 57.6 L/h-m<sup>2</sup>. The fluid properties were considered as constant with a 1052 kg/m<sup>3</sup> density and a specific heat of 3.6 kJ/kg-K.

### First Results

For validation purpose, only the experimental data recorded from January 1 to May 16 (last day of heating) were used. The model accuracy is assessed by comparing the measured and simulated useful energy gain, assuming that the inlet temperature and flowrate are known. Figure 7 shows the monthly error obtained with coefficients from Table 1 for different wind speeds used in the coefficient  $F_{rU_1}$ .

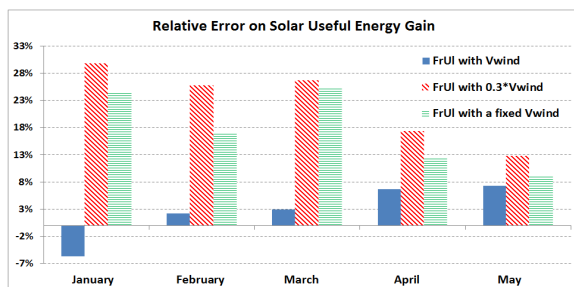


Figure 7: Monthly error on solar energy gain.

Three options are compared: the wind speed measured at the weather station in Melun (as is), the same wind speed with a multiplication factor of 0.3 as in Burch et al. (2005), and a constant wind speed of 2.4 m/s. The results based on the test report coefficients give better results with the uncorrected weather station wind speed.

Figure 8 shows that the outlet temperature calculated by TRNSYS falls within an interval of +/- 2 °C around the measured output temperature. Larger differences are observed on a few occasions. In particular, the group of data points below the interval between 17 and 27 °C has been identified as coming from 10 days (May 13 to May 23) and probably results from special experimental circumstances not accounted for in the model. One possible source of error is that the collector model does not account for condensation when the surface temperature of the collector is below the ambient dewpoint temperature. Perers (2006) has recently proposed an improved model to take this into account.

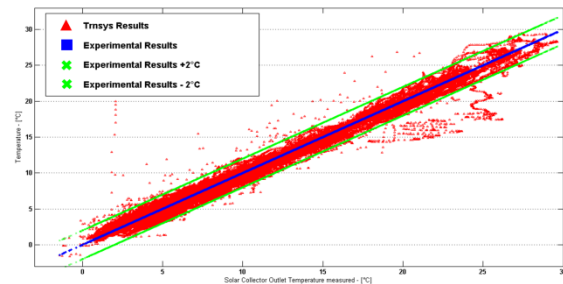


Figure 8: Simulated vs. experimental collector outlet temperature (test report parameters)

### Parameter identification

Several combinations of solar coefficients have been tested through more than 100 TRNSYS simulations. For instance, Figure 9 shows how the modelling error changes when  $a_0$  and  $a_1$  are varied. The coefficients  $b_0$  and  $b_1$  are respectively fixed to 21 W/m<sup>2</sup>·°C and 2.0 W-s/m<sup>3</sup>·°C.

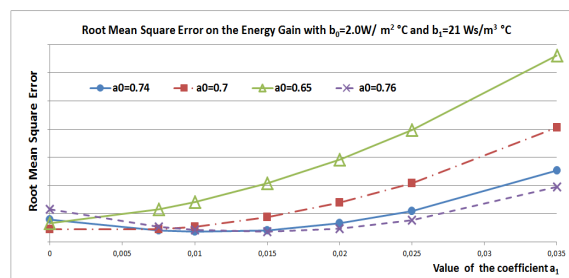


Figure 9: Example of Solar coefficients tested

Table 2 shows the final parameters (based on gross area) that have been found to minimize the root mean square error for the solar energy gain.

Table 2: Collector parameters after identification.

Parameter	Value	Unit
$a_0$	0.74	-
$a_1$	0.01	s/m
$b_0$	21	$W/m^2 \cdot ^\circ C$
$b_1$	2.0	$J/m^3 \cdot ^\circ C$

Figure 10 shows the same results as Figure 8 with the identified parameters. The fit between model results and experimental data is improved, but the results show that the model could probably be refined

further. Nevertheless, the fit obtained with the parameters in Table 2 was considered to be acceptable given the other uncertainties in the model.

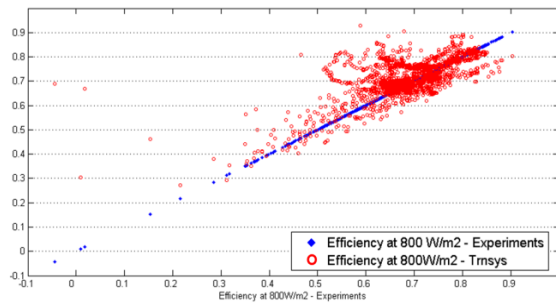


Figure 10: Simulated vs. experimental collector outlet temperature (identified parameters)

### HEAT PUMP MODEL VALIDATION

TRNSYS Type 927 from the TESS libraries (TESS, 2010) is used to model the heat pump. It uses a performance map to calculate the performance (COP and heating capacity) in heating mode (Geminoux, 2009). The performance map was adapted to match the measured COP values.

Figure 11 shows the 1-min COP values for all data points with a load-side Leaving Fluid Temperature (LWT) within 1 °C of 40 °C. The experimental and simulated COP values are plotted versus the source-side Entering Fluid Temperature, EFT.

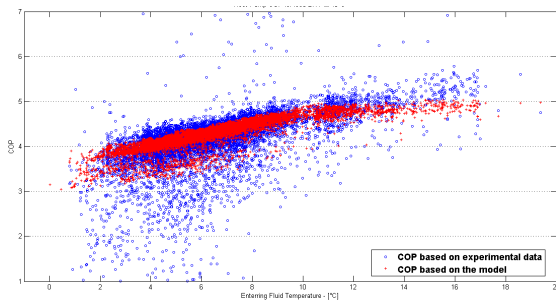


Figure 11: COP vs source EFT, load LWT of 40°C

Figure 12 shows the same results for a load-side EFT of 50 °C. Start-up and shutdown phenomena are not modeled by Type 927, which explains large differences for some time steps, but the adapted performance map matches the experimental data with a good accuracy for steady-state regime.

Figure 13 shows the daily COP values (experimental and simulated). The differences are within a few percents except for the end of the testing period (the large drop in measured COP results from an electrical fault on day 159).

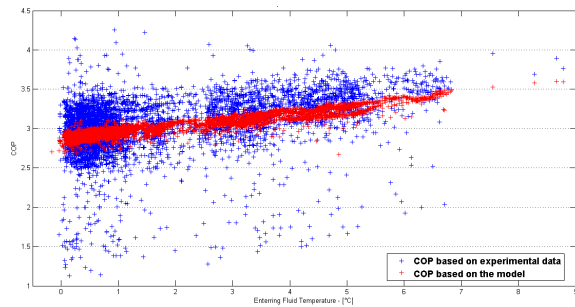


Figure 12: COP vs source EFT, load LWT of 50°C.

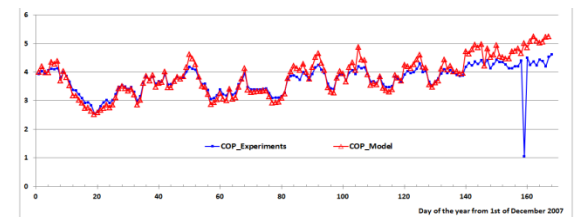


Figure 13: Simulated and experimental daily COP.

### MODEL OF A TYPICAL FRENCH OFFICE BUILDING

With around 69 MTOE consumed in 2009, e.g. 44% of the total French consumption of final energy, the built sector is the largest contributor to the country energy use. This translates into 20 % of the CO<sub>2</sub> emissions, because of the large share of nuclear energy in electricity production. (ADEME, 2010)

Office buildings in particular make a significant contribution. ADEME (2005) estimated that, on the average, a French office building equipped with air conditioning uses 127 kWh/m<sup>2</sup> for heating and 58 kWh/m<sup>2</sup> are required for cooling (net energy delivered to / removed from the zone). However, a significant fraction of office buildings are not equipped with air conditioning and rely on natural and/or forced ventilation in summer.

In this paper, a typical building presented in Filfli (2006) is used to assess the potential of SAHP systems. A typical floor plan is shown in Figure 14. The original building has 12 identical floors of 1250 m<sup>2</sup> each, and it has been reduced to 3 identical floors for this study.

Envelope parameters were selected to match the French energy regulation policy that was in force between 2000 and 2005. Table 3 shows the level of insulation assumed for opaque walls and windows (10% was added to all coefficients to account for coldbridges).

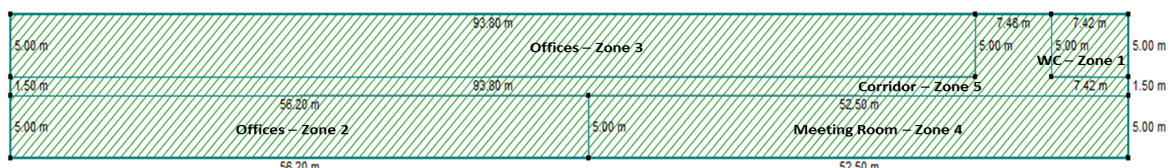


Figure 14: The building plan used to model a typical French building

Table 3: Building heat loss coefficients

Surface Type	Value	Units
Walls	0.46	W/m <sup>2</sup> -K
Roof	0.35	W/m <sup>2</sup> -K
Low Floor	0.36	W/m <sup>2</sup> -K
Glazing	3.02	W/m <sup>2</sup> -K

Occupancy schedules and internal gains assumptions are taken from Filfli (2006). Lighting density is 10 W/m<sup>2</sup>. Table 4 shows some of the modelling assumptions.

Table 4: Main parameters used for internal gains.

Zone	Area ratio	Occupancy (persons)	Computers
WC	3%	1	0
Offices 2	22%	23	18
Offices 3	28%	39	31
Meeting	21%	74	0
Corridor	16%	1	1

## Results

For the typical weather of Trappes, (30 km South West of Paris) the building heating load (net energy delivered to the zone) is 351 MWh, or 94 kWh/m<sup>2</sup>. This value is lower than the average of the building stock (125 kWh/m<sup>2</sup>). This was to be expected since the simulated building is better insulated than the building stock, being representative of new build.

Figure 15 describes the hourly loads for the three floors with a heating peak load of 284 kW. Cooling loads were calculated by the model and are shown in the Figure but they are not accounted for in the system simulation, since the building is not equipped with air conditioning

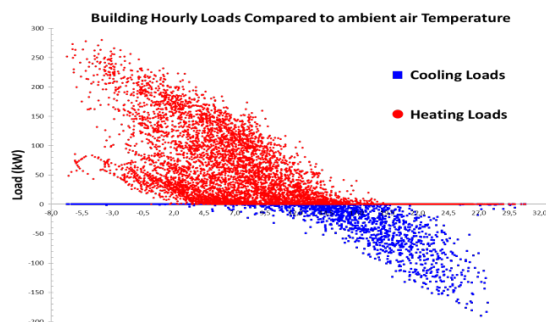


Figure 15: Hourly Loads vs.  $T_{amb}$

## SAGSHP SYSTEM WITH UNGLAZED COLLECTORS

In this section of the paper, we compare the capital cost of a conventional GSHP system designed for the office building described above to the capital cost of

an SAGSHP system using unglazed solar collectors. The building and different systems are modelled in TRNSYS using the validated component models.

### Model of Ground Heat Exchanger

Vertical boreholes with U-tube heat exchangers are commonly used in ground source heat pump applications. They are well suited to buildings with high loads and limited available land area. For this study, the depth of vertical boreholes is fixed at 100 m and their diameter at 0.15 m. These parameters are representative of typical systems in France. The top of the ground heat exchanger is 1m below the surface of the ground and the boreholes are filled with a grout material, typically a mixture of sand and bentonite. Ground properties estimated from a thermal response test performed at the EDF R&D center are used in this study: thermal conductivity is 2.0 W/m-K and thermal diffusivity is 0.05 m<sup>2</sup>/day (Cauret et al, 2009). The weather conditions are taken for a typical year in Trappes. (Meteotest, 2010). The GHX is modelled using TESS Type 557, known as the DST (Duct Storage) model (TESS, 2010). This model assumes that the boreholes are placed uniformly within a cylindrical storage volume of ground. The borehole spacing is set at 6 m. Table 5 shows the main parameters in the model.

Table 5: GHX main parameters

Parameter	Value	Units
Pipe Inner Radius	0.0137	m
Pipe Outer Radius	0.0167	m
Distance between pipes	0.10	m
Pipe Thermal Conductivity	0.42	W/m-K
Grout Thermal Conductivity	1.5	W/m-K
Ground Thermal Conductivity	2.0	W/m-K
Ground Thermal Diffusivity	0.05	m <sup>2</sup> /day
Initial Ground Temperature	12	°C
Investment Costs	100	€/m

### Solar system

The solar collector parameters are the identified values shown in Table 2. A controller continuously compares the solar outlet temperature with the GHX outlet temperature and circulates the fluid through the solar collectors when there is a difference of 0.5°C or more. This control strategy is the same as the one implemented during the experiments at the EDF facility. The solar auxiliary pump drives the solar nominal flow rate with a power of 21 W/m<sup>2</sup> of collectors. This is assumed to be enough to overcome the head losses through the underground loop.

### Capital costs

The cost of 100 €/m taken for the ground exchangers is an average based on French figures. For solar collectors, a value as low as 60 €/m<sup>2</sup> is sometimes reported but actual quoted values for the unglazed collectors selected in the study were found to be as high as 100 €/m<sup>2</sup> in some cases. Solar and GHE costs include system installation but exclude taxes.

### Design criterion

In heating-only GSHP systems, the main design consideration are that the ground return temperature (heat pump entering fluid temperature on the source side) must remain above the acceptable limits at all times. Typically the lowest temperature will occur during the last year of operation. A 20 year period was considered in this study, and the lowest acceptable return temperature from the ground is taken as -1 °C. The different designs are obtained by running successive simulations with different GHX lengths until the criterion is met.

### Results

Without solar collectors, 89 boreholes are required for a capital cost of 890 k€ and a land occupancy of 2775 m<sup>2</sup>, e.g. more than twice the building footprint. The average ground temperature decreases by 0.45 °C per year of operation, leading to COP degradation over the years (see below). Adding solar collectors decreases the required borehole length and the capital costs, as shown in Figure 16.

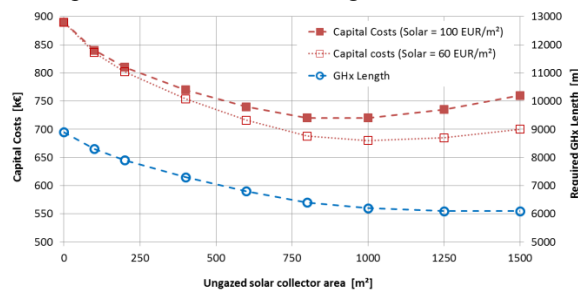


Figure 16: GHX Length and capital costs vs. solar collector area

Figure 16 shows that capital costs present a minimum value for a solar collector area between 750 m<sup>2</sup> and 1000 m<sup>2</sup> depending on the assumed solar collector cost. A value of 1000 m<sup>2</sup> (corresponding to 60 €/m<sup>2</sup>) is used in the following for the sake of simplicity. With that collector area, the borehole length is reduced by 30% and the capital costs are reduced by 23%. The surface area required for boreholes is also reduced by 30 % since a constant length is assumed. Additional surface area is required for solar collectors, and the combined area is in fact slightly higher than for the “pure” GSHP system. But solar collectors can be installed on the roof of the building.

Figure 17 shows that the minimum heat pump entering fluid temperature is lower for the SAGSHP during the first year, but the temperature drop from

year to year is lower and both the GSHP and the SAGSHP reach the same minimum temperature (-1 °C, the design value) after 20 years. The solar collectors provide the most energy in summer.

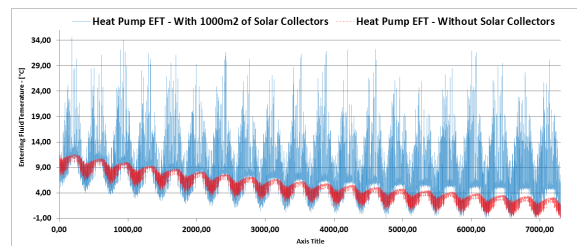


Figure 17: Heat pump EFT with and without solar collectors

Figure 18 shows that the solar collectors also have a positive impact on the heat pump COP, reducing the electricity consumption. But the solar collector circulating pump is also using electricity, so it is interesting to look at the overall consumption and life-cycle cost (LCC) of the systems. With an electricity cost of 0.07 €/kWh, an energy inflation rate of 10% (EIA, 2011), and a discount rate of 6%, the configuration with 1000 m<sup>2</sup> of solar collectors has higher operating costs but remains a better option over 20 years of operation. The Life-Cycle Cost (LCC) with solar is about 1 M€, 15 % lower than the LCC of the GSHP-only system. Considering a higher capital cost for solar collectors (100 €/m<sup>2</sup>), LCC savings are reduced to 13 %.

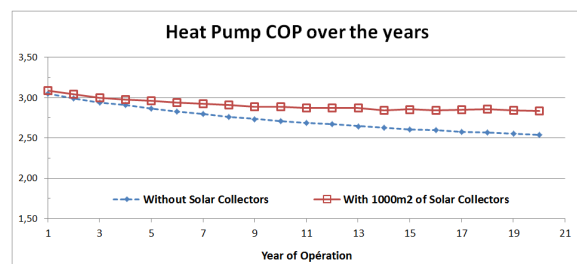


Figure 18: Heat pump COP evolution over the years

## DISCUSSION AND CONCLUSIONS

This paper presents a study for examining the viability of solar assisted ground source heat pump (ASGSHP) systems that use unglazed solar collectors in heating-only buildings. An experimental facility located at EDF R&D center was used to validate a model of heat pump and unglazed solar collector and the agreements between the models and the experiments are generally good. Space heating loads for a typical French office building near Paris were used to compare GSHP and SAGSHP system configurations. The study concludes that the SAGSHP system can deliver capital cost savings of 23% and LCC savings of 15% over 20 years. These numbers depend on local economic parameters but are within the range found in previous studies (see Introduction).

One of the main assumptions in the study is that the building is not equipped with air conditioning. While

this is representative of a large number of office buildings in France, further work is required to assess the potential benefits of SAGSHP systems in heating-dominated (and not heating-only) buildings. One of the main issues with the current system configuration and controls would be that solar recharge in summer would at best reduce the heat pump performance in cooling mode, and at worst prevent the heat pump from operating. In this study horizontal collectors have been assumed because this is the most cost-effective option if collectors are installed on a flat roof and solar heat can be used in summer. Tilted collectors could be more interesting if solar heat is undesirable in summer, e.g. if it competes with cooling.

Different design methods will also be explored. In this paper we assume that the borehole length is adapted to result in the same ground return temperature after 20 years when solar collectors are added. Other design methods have been proposed, e.g. balancing the yearly load (Chiasson, 2009). Other tertiary or commercial building types (e.g. health sector) should also be studied in various locations in France.

## REFERENCES

- ADEME, 2005. Les chiffres clés du bâtiment 2005. Agence de l'Environnement et de la Maîtrise de l'Energie, France.
- ADEME, 2010. Les chiffres clés du bâtiment 2010. Agence de l'Environnement et de la Maîtrise de l'Energie, France.
- Blum, P., Campillo, G., and Kölbl, T. 2011. Techno-economic and spatial analysis of vertical Ground source heat pump systems in Germany. *Energy*, 36, pp. 3002–3011.
- Burch, J., Salasovitch, J., and Hillman, T. 2005. An assessment of unglazed solar domestic water heaters. Presented at the ISES Solar World Congress, Orlando, Florida. NREL /CP-550-37759. National Renewable Energy Laboratory, Golden, CO.
- Cauret O. and Teuillière C. 2007. Programme d'essais de capteurs hélio-atmosphériques couplés aux capteurs compacts en tranchée sur la plateforme Climat naturel. Technical report, EDF R&D, France.
- Cauret, O. and Bernier, M. 2009. Experimental Validation of an Underground Compact Collector Model. In Proceedings of Effstock 2009, June 14-17, Stockholm, Sweden.
- CEN, 2005. Thermal solar systems and components – solar collectors – Part 2: Test methods,” European Committee for Standardization, EN 12975-2.
- Chiasson, A.D., and Yavuzturk, C. 2003. Assessment of the performance of hybrid geothermal heat pump systems with solar thermal collectors. *ASHRAE Transactions*, 109 (2), pp. 487–500.
- Chiasson, A.D., and Yavuzturk, C. 2009. A Design Tool for Hybrid Geothermal Heat Pump Systems in Heating-Dominated Buildings. *ASHRAE Transactions*, 115, part 2, pp. 60–73.
- CSTB. 2008. Avis Technique 14/08-1238 Capteur Solaire sans vitrage, Solarpool, Héliopac. Centre Scientifique et Technique du Bâtiment, Marne la Vallée, France.
- Duffie, J.A., and Beckman, W. A. 2006. *Solar Engineering of Thermal Processes*, 3rd ed. Wiley, Hoboken, NJ.
- EERE, 2010. EnergyPlus Energy Simulation Software – Real-time Weather Data. <http://bit.ly/kAtCEo>. US Department of Energy, Energy Efficiency and Renewable Energy.
- EIA. 2011. U.S. Energy Information Administration - International Electricity Prices and Fuel Costs - Electricity Prices for Industry.
- Filfli, S. 2006. Optimisation bâtiment/système pour minimiser les consommations dues à la climatisation. PhD thesis, École des Mines de Paris, France.
- Geminox. 2009. Pompes à chaleur modèle ECOLANE SE – 9C, pp 33- 37. Geminox, Saint-Thégonnec, France.
- Kadir Bakirci, K., Ozyurt, O., Comakli, K. and Comakli O. 2011. Energy analysis of a solar-ground source heat pump system with vertical closed-loop for heating applications. *Energy*, 36, pp. 3224–3232.
- Meteotest, 2010. Meteonorm software, version 6.1. Meteotest, Switzerland.
- Ozgener O. and Hepbasli, A. 2005. Performance analysis of a solar-assisted ground-source heat pump system for greenhouse heating: an experimental study. *Building and Environment*, 40, pp. 1040–1050.
- Perers, 2006. A Dynamic collector model for simulation of the operation below the dewpoint in heat pump systems. Proceedings of the International Conference EuroSun 2006, Glasgow, 27-30 June.
- Rad, F.M., Fung, A.S. and Leong W.H. 2009. Combined solar thermal and ground source heat pump system. In proceedings of Building Simulation 2009, the 11th International Building Performance Simulation Association Conference, Glasgow, Scotland, pp. 2297–2305.
- TESS, 2010. TESS Libraries version 17.01. Thermal energy Systems Specialists, Madison, WI.